

# The $\beta$ Fermi-Pasta-Ulam-Tsingou recurrence problem

Cite as: Chaos **29**, 113107 (2019); <https://doi.org/10.1063/1.5122972>

Submitted: 01 August 2019 . Accepted: 21 October 2019 . Published Online: 06 November 2019

Salvatore D. Pace , Kevin A. Reiss , and David K. Campbell 



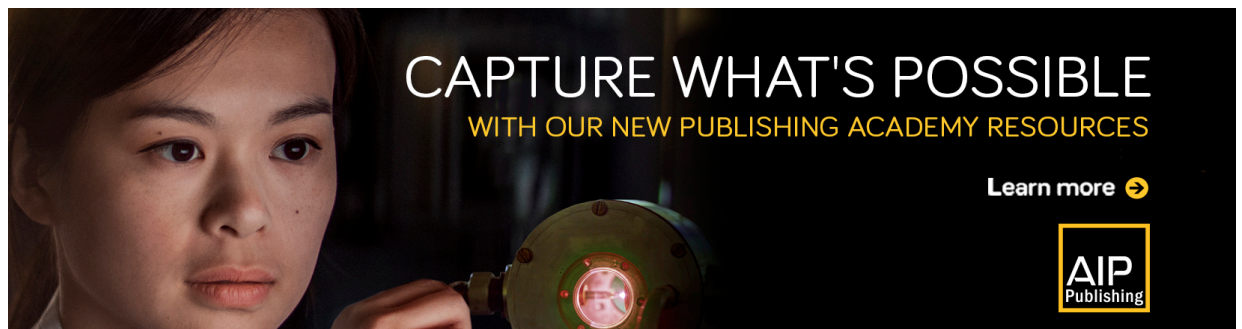
[View Online](#)



[Export Citation](#)



[CrossMark](#)



CAPTURE WHAT'S POSSIBLE  
WITH OUR NEW PUBLISHING ACADEMY RESOURCES

[Learn more](#) 



# The $\beta$ Fermi-Pasta-Ulam-Tsingou recurrence problem

Cite as: Chaos 29, 113107 (2019); doi: 10.1063/1.5122972

Submitted: 1 August 2019 · Accepted: 21 October 2019 ·

Published Online: 6 November 2019



View Online



Export Citation



CrossMark

Salvatore D. Pace,  Kevin A. Reiss,  and David K. Campbell 

## AFFILIATIONS

Department of Physics, Boston University, Boston, Massachusetts 02215, USA

## ABSTRACT

We perform a thorough investigation of the first Fermi-Pasta-Ulam-Tsingou (FPUT) recurrence in the  $\beta$ -FPUT chain for both positive and negative  $\beta$ . We show numerically that the rescaled FPUT recurrence time  $T_r = t_r/(N + 1)^3$  depends, for large  $N$ , only on the parameter  $S \equiv E\beta(N + 1)$ . Our numerics also reveal that for small  $|S|$ ,  $T_r$  is linear in  $S$  with positive slope for both positive and negative  $\beta$ . For large  $|S|$ ,  $T_r$  is proportional to  $|S|^{-1/2}$  for both positive and negative  $\beta$  but with different multiplicative constants. We numerically study the continuum limit and find that the recurrence time closely follows the  $|S|^{-1/2}$  scaling and can be interpreted in terms of solitons, as in the case of the KdV equation for the  $\alpha$  chain. The difference in the multiplicative factors between positive and negative  $\beta$  arises from soliton-kink interactions that exist only in the negative  $\beta$  case. We complement our numerical results with analytical considerations in the nearly linear regime (small  $|S|$ ) and in the highly nonlinear regime (large  $|S|$ ). For the former, we extend previous results using a shifted-frequency perturbation theory and find a closed form for  $T_r$  that depends only on  $S$ . In the latter regime, we show that  $T_r \propto |S|^{-1/2}$  is predicted by the soliton theory in the continuum limit. We then investigate the existence of the FPUT recurrences and show that their disappearance surprisingly depends only on  $E\beta$  for large  $N$ , not  $S$ . Finally, we end by discussing the striking differences in the amount of energy mixing between positive and negative  $\beta$  and offer some remarks on the thermodynamic limit.

Published under license by AIP Publishing. <https://doi.org/10.1063/1.5122972>

In 1953, Enrico Fermi, John Pasta, Stanislaw Ulam, and Mary Tsingou used computer-based simulations on the MANIAC I at the Los Alamos Scientific Laboratory to study the equilibration rate of masses coupled by nonlinear springs. Since their seminal paper that surprisingly showed that the system did not approach equilibrium and instead exhibited near recurrences to its initial configuration,<sup>1</sup> researchers are still investigating the now called Fermi-Pasta-Ulam-Tsingou (FPUT) problem. This paper studies the scaling and existence of the FPUT recurrences in the  $\beta$ -FPUT chain for both negative and positive  $\beta$ . We find that a rescaled recurrence time depends only on a single parameter,  $S$ , which is based on the system size, initial energy  $E$ , and the nonlinear parameter  $\beta$ . The scaling can be understood using a perturbation theory for small  $S$  and studying solitary waves that exist in the continuum limit for large  $S$ . We find that the existence of the FPUT recurrences, for large systems, depends only on a critical values of  $E\beta$ , which differ based on the sign of  $\beta$ . These results strongly suggest that further studies on the  $\beta$ -FPUT chain be done for negative  $\beta$ .

## I. INTRODUCTION

Fermi, Pasta, Ulam, and Tsingou (FPUT) numerically investigated the dynamics of a homogeneous anharmonic chain initialized far from equilibrium to study the effect of nonlinear interactions on thermal conductivity and ergodicity in solids.<sup>1</sup> To their surprise, their computational results showed that within observed time scales, the system did not obtain energy equipartition among normal modes. Instead, when the first normal mode was initially excited, they observed energy flow among only the lowest normal modes with periodic near-recurrences to the initial state. These “FPUT recurrences” and the questions they raise about how systems approach equilibrium have puzzled and challenged researchers for more than 60 years.<sup>2-5</sup>

Since their discovery, three seemingly different pictures have been developed to explain the cause of the recurrences in what is now called the FPUT chain. First revealed by a shifted-frequency perturbation theory, the FPUT recurrences occur because of near resonances between perturbatively defined nonlinear frequencies.<sup>6,7</sup> Next, in an interpreted continuum limit, the equations of motion

become a partial differential equation with solitary wave solutions called “solitons.” In this limit, FPUT’s initial conditions break up into multiple solitons moving at different velocities, and the FPUT recurrence occurs when the solitons overlap in the same configuration they started in Ref. 8. Finally, the third explanation comes from time-periodic localized structures in normal mode space called  $q$ -breathers,<sup>9</sup> or more generally  $q$ -tori,<sup>10</sup> which are exact solutions of the FPUT chain’s equations of motion. The FPUT recurrences occur because the trajectories of long-wavelength initial excitations are perturbations of the  $q$ -tori orbits.

Much of the previous work—in particular, that dealing with the soliton approach—has focused on the  $\alpha$ -FPUT chain, in which the nonlinear term in the Hamiltonian is proportional to the cube of the difference in the positions of neighboring masses. In the present work, we investigate the FPUT recurrence and its scaling in the  $\beta$ -FPUT chain, in which the nonlinear term in the Hamiltonian is proportional to the fourth power of the difference in the positions of neighboring masses. Indeed, while there have been numerous studies on the FPUT recurrences in the  $\alpha$ -FPUT chain,<sup>11–14</sup> to our knowledge, there has yet to be a complete study on them in the  $\beta$ -FPUT chain. In later sections of this article, we offer detailed reasons why this situation has occurred but in brief, it has to do with instabilities known to exist both on the lattice and in continuum limit,<sup>15</sup> which make numerical studies of the  $\beta$ -FPUT recurrences challenging,<sup>16,17</sup> as well as peculiarities in the method of solution for the continuum model. We will clarify these somewhat cryptic comments later.

In the majority of previous studies of the  $\beta$ -FPUT chain, the quartic interactions were attractive ( $\beta > 0$ ) rather than repulsive ( $\beta < 0$ ). This is likely because negative  $\beta$  causes saddle points in the potential and therefore, “large enough” initial energies will lead to trajectories blowing up. The positive  $\beta$ -FPUT’s potential is instead completely bounded from below. However, it is still interesting to study unbounded potentials for energies below the saddle points. Indeed, in the  $\alpha$ -FPUT chain, such saddle points always exist because the nonlinear interaction is cubic. Moreover, as noted by previous studies,<sup>18</sup> for energies below any blowup, the dynamics for  $\beta < 0$  are not a trivial extension of the  $\beta > 0$  results and should be independently considered. For example, the solitons which form in the continuum limit for  $\beta > 0$  are exponentially unstable, whereas for  $\beta < 0$ , they are (perhaps surprisingly) stable.<sup>15</sup> Furthermore, the dynamics of a one-dimensional Bose gas in the quantum rotor regime maps onto the  $\beta$ -FPUT chain with  $\beta < 0$ .<sup>19</sup> Hence, a primary focus of our study will be the comparison of the FPUT recurrences between the conventional  $\beta > 0$  and atypical  $\beta < 0$ .

We note that along with their central role in FPUT chains, FPUT recurrences have also been found and studied in numerous other theoretical models and also observed experimentally in various physical systems. Examples of the former include electron-phonon interactions,<sup>20</sup> interacting Bose-Einstein condensates,<sup>19,21</sup> ion waves,<sup>22</sup> and anti-de Sitter spacetime.<sup>23,24</sup> The latter involves experimental demonstrations with electrical networks,<sup>25</sup> plasmas,<sup>26</sup> deep-water waves,<sup>27</sup> silica optical fibers,<sup>28</sup> magnetic film strips,<sup>29,30</sup> and optics in a photorefractive crystal.<sup>31</sup>

The outline of the paper is as follows. In Sec. II, we introduce the  $\beta$ -FPUT chain and show how its continuum limit becomes the well-known modified Korteweg–de Vries (mKdV) equation. Then, in Sec. III we report and discuss our numerical determination of the

scaling in time of the FPUT recurrences, importantly showing that a rescaled FPUT recurrence time depends, for large  $N$ , only on the parameter  $S \equiv E\beta(N+1)$ . In Sec. IV, we extend the results from Ref. 7 and present analytic results for the FPUT recurrence time in the nearly linear regime as a function of  $S$  only. In Sec. V, we investigate numerically the recurrence of the initial state in the mKdV equation and examine the role played by solitons. Next, in Sec. VI, we explore the highly nonlinear regime and find an analytical expression for the FPUT recurrence time using the soliton velocities in the continuum. In Sec. VII, we look at the dependence of the formation of the first FPUT recurrence on lattice parameters. Finally, in Sec. VIII, we offer concluding remarks and highlight some open questions.

## II. THE $\beta$ -FPUT CHAIN AND ITS CONTINUUM LIMIT

The  $\beta$ -FPUT chain is described by the classical Hamiltonian

$$H = \sum_{n=0}^N \frac{p_n^2}{2m} + \frac{k_2}{2} (q_{n+1} - q_n)^2 + \frac{k_4}{4} (q_{n+1} - q_n)^4, \quad (1)$$

where  $q_n$  and  $p_n$  are, respectively, the displacement from rest and canonical momentum of site  $n$ ,  $N$  is the number of active masses,  $m$  is the mass, and  $k_2$  and  $k_4$  are weights of the quadratic and quartic interactions, respectively. Using the canonical transformation

$$\begin{bmatrix} q_n \\ p_n \end{bmatrix} = \sqrt{\frac{2}{N+1}} \sum_{k=1}^N \begin{bmatrix} Q_k \\ P_k \end{bmatrix} \sin\left(\frac{nk\pi}{N+1}\right), \quad (2)$$

we diagonalize the quadratic term of the Hamiltonian and transform to normal mode coordinates  $(Q_k, P_k)$ . With this, Eq. (1) becomes

$$H = \sum_{k=1}^N \frac{P_k^2}{2m} + \frac{k_2 \omega_k^2 Q_k^2}{2} + \frac{k_4}{4} \sum_{i,j,l=1}^N C_{kijl} Q_k Q_i Q_j Q_l, \quad (3)$$

where the normal mode frequencies are

$$\omega_k = 2 \sin\left(\frac{k\pi}{2(N+1)}\right) \quad (4)$$

and the coupling constants are<sup>32</sup>

$$C_{kijl} = \frac{\omega_k \omega_i \omega_j \omega_l}{2(N+1)} \sum_{\pm} [\delta_{k,\pm j \pm l \pm m} - \delta_{k,\pm j \pm l \pm m, \pm 2(N+1)}]. \quad (5)$$

The sum  $\sum_{\pm}$  in Eq. (5) is over all possible combinations of plus and minus signs in the  $\pm$ s of the Kronecker delta functions,  $\delta_{i,j}$ .

From Hamilton’s equations ( $\dot{q} = \partial_p H$ ,  $\dot{p} = -\partial_q H$ ), the real space equations of motion are

$$\ddot{q}_n = q_{n+1} + q_{n-1} - 2q_n + b|\beta|[(q_{n+1} - q_n)^3 - (q_n - q_{n-1})^3], \quad (6)$$

where we have defined  $\beta \equiv k_4/k_2$  and rescaled time by the multiplicative constant  $\sqrt{k_2/m}$ . Furthermore, because we will be considering both  $\beta > 0$  and  $\beta < 0$ , we have taken the absolute value of  $\beta$  and have introduced  $b \equiv \text{sgn}(\beta)$ . In the continuum limit, in which  $N$  goes to infinity while the lattice spacing,  $a$ , goes to zero such that the length of our chain,  $L = a(N+1)$ , is fixed, the displacement

variables  $\{q_n(t)\}$  become a field  $q(x, t)$ , with

$$q_n(t) \equiv q(na, t). \tag{7}$$

To take the continuum limit, we Taylor expand  $q_{n\pm 1}(t)$  to fourth order in  $a$ ,

$$q_{n\pm 1}(t) = q \pm aq_x + \frac{a^2}{2}q_{xx} \pm \frac{a^3}{6}q_{xxx} + \frac{a^4}{24}q_{xxxx}, \tag{8}$$

where we employ the notation  $q(x, t) \equiv q$  and use subscripts to denote partial differentiation. Plugging this in the equations of motion, dropping fifth-order terms in  $a$ , and then simplifying we find

$$\ddot{q} = a^2 (q_{xx} + b\varepsilon(q_x)^2q_{xx} + \zeta\varepsilon q_{xxxx}), \tag{9}$$

where we have defined the variables  $\varepsilon = 3|\beta|a^2$  and  $\zeta = 1/(36|\beta|)$ . Using the multiple time scale expansion and then considering the asymptotic solution of a right-going wave,  $q(x, t) \sim F(\xi, \tau)$ , where  $\xi = x - at$  and  $\tau = \varepsilon at/2$ .<sup>33</sup> Plugging this into Eq. (9) gives

$$F_{\xi, \tau} + b(F_{\xi})^2F_{\xi\xi} + \zeta F_{\xi\xi\xi\xi} = 0. \tag{10}$$

Introducing a new field  $\phi = F_{\xi}$ , we arrive at the standard form for the mKdV equation

$$\phi_{\tau} + b\phi_{\xi}\phi^2 + \zeta\phi_{\xi\xi\xi} = 0. \tag{11}$$

In the literature, the mKdV equation is called the “focusing” (“defocusing”) mKdV equation when  $b = 1$  ( $b = -1$ ).

Let us stress that the mKdV equation does not exactly model the dynamics of the  $\beta$ -FPUT chain, as the multiple time scale expansion will break down on large time scales. Nevertheless, as shown in numerous studies in the  $\alpha$ -FPUT chain (see Refs. 12–14, 22, 34, and 35), the soliton dynamics in the KdV equation is a reliable tool to study the lattice dynamics for a large range of parameters, in particular, at large  $N$ .

The initial conditions on the lattice are  $q_n(0) = A\sin(n\pi/(N + 1))$ , and we will use fixed boundary conditions,  $q_0 = q_{N+1} = 0$ . Because the equations of motion of the  $\beta$ -FPUT chain preserve odd symmetry about the chain’s center, the dynamics of our chain will be equivalent to a chain with  $2N + 2$  active masses and the same initial conditions but under the periodic boundary conditions  $q_0 = q_{2N+2}$ .<sup>11</sup> In the continuum limit, we will take advantage of this and consider  $\xi \in [0, 2L]$  with  $\phi(0, \tau) = \phi(2L, \tau)$ . The initial conditions on the lattice will become  $\phi(\xi, 0) \sim q_x(x, 0)/2 = A\kappa \cos(\kappa\xi)/2$ , where  $\kappa = \pi/L$ . We have divided by two to take into account that the mKdV equation only describes the right-going waves.

### III. NUMERICAL SCALING OF FPUT RECURRENCE TIME

In this section, we report our numerical results for the dependence of the FPUT recurrence time on the parameters of the  $\beta$ -FPUT chain ( $N$ ,  $\beta$ , and the energy  $E$ ). Our numerics were performed using the symplectic SABA<sub>2</sub>C integrator.<sup>36</sup> This numerical scheme produces an error of  $\mathcal{O}(dt^4)$ , where  $dt$  is the numerical time step size, which we typically have set to  $dt = 0.1$ . For more details regarding the relative energy error and the explicit form of the numerical scheme for FPUT chains, see the appendix of Ref. 17.

Figure 1 shows the energy in the first nine normal modes for  $E = 0.15$ ,  $\beta = 1$ , and  $N = 127$ . These data were obtained by first numerically solving Eq. (6), applying the canonical transformation

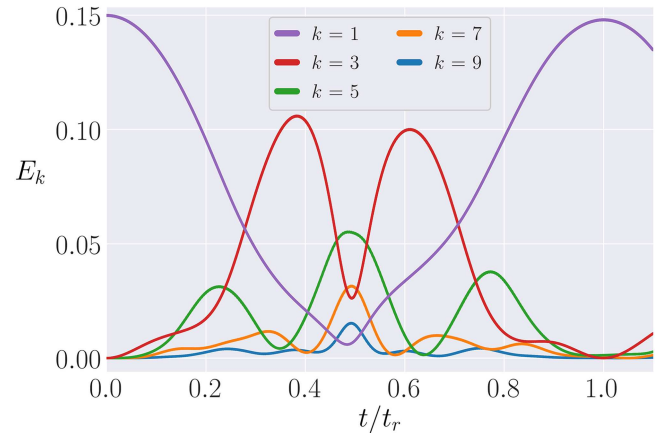


FIG. 1. Shows the modal energy dynamics for the first nine normal modes of the  $\beta$  FPUT chain with  $E = 0.15$ ,  $\beta = 1$ , and  $N = 127$ . Because of the invariance under reflection about the chain’s center, for odd normal mode initial conditions in the  $\beta$ -FPUT chain, even normal modes are never excited. We have rescaled the temporal axis by the FPUT recurrence time,  $t_r$ .

given by Eq. (2), and then using Eq. (3) to find the energy in the  $k$ th normal mode. Using the data presented in Fig. 1, we categorize the FPUT recurrence as the time where the energy in the first normal mode is a local maximum and nearly equals the total system energy. To emphasize this, we have rescaled the temporal axis in the plot by the recurrence time  $t_r$ . We note that this technique does not necessarily imply a near return to the initial configuration in the  $2^N$  dimensional phase space. For example, the energy return could be in a different phase of the fundamental period oscillation. However, we follow this definition of the FPUT recurrence to remain consistent with previous studies and to closely align with the historical focus of the FPUT problem on energy equipartition.

In the  $\alpha$ -FPUT chain, for large  $N$ , the rescaled recurrence time  $T_r \equiv t_r/(N + 1)^3$  depends only on the parameter  $R \equiv E\alpha^2(N + 1)^3$ .<sup>12,14,37</sup> Rescaling the recurrence time by  $(N + 1)^3$  comes from the perturbative result that in the large  $N$  limit, as the chain approaches the harmonic limit the FPUT recurrence time scales like  $(N + 1)^3$ .<sup>6</sup> While considering a subsystem restricted to only four consecutive normal modes of the  $\beta$ -FPUT chain with  $\beta > 0$ , De Luca *et al.* found that a limiting form of the resulting Hamiltonian depends only on the parameter  $6\beta E(N + 1)/\pi^2$ .<sup>18</sup> Thus, it is reasonable to investigate the rescaled FPUT recurrence times in the  $\beta$ -FPUT chain as a function of the parameter  $S \equiv E\beta(N + 1)$ . This parameter importantly takes into account that we expect there should be a difference in the dynamics based on the sign of  $\beta$ .

Let us first consider the more conventional  $\beta > 0$  case. Figure 2 shows our numerical results on a log-log plot for the rescaled recurrence time,  $T_r$ , as a function of  $S$ . We start in the regime of small  $|S|$  and fit our data with a linear function. We find that for  $0 < S \lesssim 1$ , the data goes like

$$T_r = 0.2024 + 0.0227S. \tag{12}$$

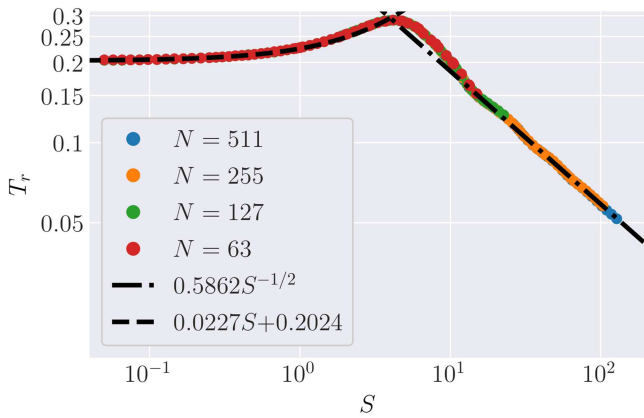


**FIG. 2.** Numerical data for the rescaled FPUT recurrence time  $T_r \equiv t_r/(N + 1)^3$  as a function of  $S \equiv E\beta(N + 1)$  on a log-log plot for the  $\beta$ -FPUT chain with  $\beta > 0$ . For the largest system size, the data extend over the full range of  $S$  shown in the plot. For smaller sizes, the data stop at certain values of  $S$  for reasons discussed in the text. The two dashed lines are numerically generated fits.

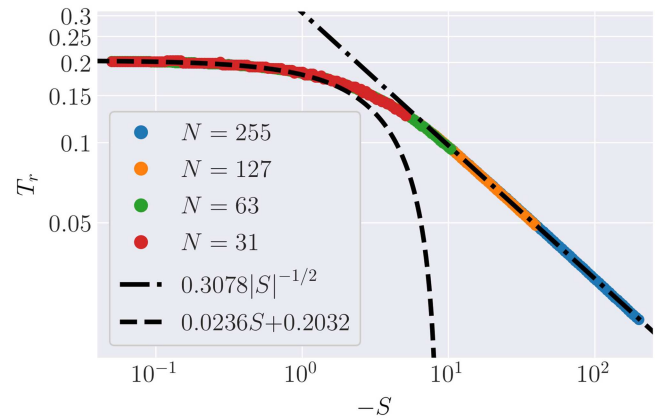


**FIG. 3.** Numerical data of the rescaled FPUT recurrence time  $T_r \equiv t_r/(N + 1)^3$  as a function of  $S \equiv E\beta(N + 1)$  on a log-log plot for the  $\beta$ -FPUT chain with  $\beta < 0$ . For the largest system size, the data extend over the full range of  $-S$  shown in the plot. For smaller sizes, the data stop at certain values of  $-S$  for reasons discussed in the text. The two dashed lines are numerically generated fits.

For large  $|S|$ , as is clear from the plot, the rescaled FPUT recurrence time exhibits power-law scaling. Fitting the numerical data gives the expression

$$T_r = \frac{0.5862}{\sqrt{S}}, \tag{13}$$

which provides an accurate fit for  $S \gtrsim 30$ .

Moving on to  $\beta < 0$ , Fig. 3 shows the numerical results of the rescaled FPUT recurrence time. For small  $|S|$ , we again fit our data with a linear function and find that for  $-0.5 \lesssim S < 0$ ,

$$T_r = 0.2032 + 0.0236S. \tag{14}$$

For large  $|S|$ , we find that once again the rescaled recurrence time shows power-law scaling. Numerically fitting this region gives that for  $S \lesssim -12$ ,

$$T_r = \frac{0.3078}{\sqrt{|S|}}. \tag{15}$$

So, for both positive and negative  $\beta$ , the rescaled FPUT recurrence time at large  $|S|$  is proportional to  $|S|^{-1/2}$ . For small  $|S|$ , the rescaled FPUT recurrence time scales linearly, smoothly transitioning between negative and positive  $\beta$ . Indeed, comparing Eqs. (12) and (14) shows that the numerical fits in this region are essentially independent of the sign of  $\beta$ . Furthermore, it is interesting to observe that the maximum value of  $T_r$  is not at zero but instead at  $S \sim 4.21$ .

Note that in both Figs. 2 and 3, the numerical results for a given  $N$  are not plotted above some value of  $|S|$ . The reasons for this differ between the two cases. When  $\beta > 0$ , this is because the FPUT recurrences simply stop forming; we will discuss this in greater detail in Sec. VII. When  $\beta < 0$ , for a given system size  $N$ , for large enough  $|S|$ , the rescaled FPUT recurrence times develop an  $N$  dependence and hence start to disagree with Fig. 3. However, for large enough system size  $N$ , the dynamics on the lattice are well modeled by the dynamics in the continuum and indeed depend only on the parameter  $S$ . This

will be evident in Secs. IV and VI where our analytical results rely asymptotically on only  $S$  when  $N$  is large. In the  $\alpha$ -FPUT chain, the threshold between “small” and “large” system sizes, and the energy at which the chain can start blowing up due to the unbounded potential are correlated.<sup>38</sup> As we show in Appendix B, the small vs large threshold for the  $\beta$ -FPUT chain with  $\beta < 0$  follows the same correlation and that the system can be considered large when  $N > 4|S| - 3$ .

Therefore, we see that as in the case of  $R$  for the  $\alpha$ -FPUT chain, for large  $N$ , the parameter  $S$  fully describes the rescaled FPUT recurrence time in the  $\beta$ -FPUT chain for both positive and negative  $\beta$ . Interestingly, while we have shown in a previous study that  $R$  describes the singularities in the periods of the higher-order recurrences (e.g., super recurrences, super-super recurrences, etc.) in the  $\alpha$ -FPUT chain, we have not found that  $S$  describes such singularities in the  $\beta$ -FPUT chain.<sup>17</sup>

#### IV. NEARLY LINEAR REGIME ANALYTICS

When  $|S|$  is small, the system is in a nearly linear regime, and its dynamics can be understood by adding perturbative corrections to the harmonic chain’s dynamics and acoustic phonon frequencies. This so-called “shifted-frequency perturbation theory” has been used to study the dynamics of both the  $\alpha$  and  $\beta$  FPUT chain for first normal mode initial excitations.<sup>6,7</sup> In this section, we look at the expression

$$t_r = \frac{2\pi}{3\Omega_1 - \Omega_3}, \tag{16}$$

found by Sholl and Henry for the FPUT recurrence time in the  $\beta$ -FPUT chain.<sup>7</sup> The  $\Omega_k$ s are nonlinear frequencies that have been calculated to second order in  $\beta$ . For more information about the perturbation scheme and how the nonlinear frequencies are constructed, we refer the reader to Appendix C.

As shown numerically in Sec. III, the rescaled FPUT recurrence time for large  $N$  is a function of only  $S \equiv E\beta(N + 1)$ . Therefore, at large  $N$ , the perturbative results should become only a function of  $S$  as well. Let us first rewrite the perturbative parameter,  $\beta$ , as a function of  $S$  and  $N$ . Sholl and Henry considered the initial conditions  $Q_k(0) = \delta_{k,1}$ , which corresponds to real space initial conditions  $q_n = \sqrt{2/(N + 1)}\sin(n\pi/(N + 1))$ . Using Eq. (A2) from Appendix A, this corresponds to initial conditions with

$$S = \frac{\omega_1^2 \beta(N + 1)}{2} \left( 1 + \frac{3\beta\omega_1^2}{4(N + 1)} \right). \quad (17)$$

Therefore, by solving for  $\beta$  in the above equation, we can replace the  $\beta$ s in the definition of the nonlinear frequencies and find the FPUT recurrence time as a function of only  $S$  and  $N$ . After some involved calculations with Mathematica™, we find that the denominator of Eq. (16) can be written as

$$3\Omega_1 - \Omega_3 = \frac{1}{(N + 1)^3} \left( \frac{46\pi^3}{3} + \frac{15\pi S}{16} + \frac{240\pi^5}{3S - 16\pi^2} + \frac{16\pi^5}{24\pi^2 - 27S} \right) + \mathcal{O}\left(\frac{1}{(N + 1)^5}\right). \quad (18)$$

Dropping the fifth-order terms, inserting this into Eq. (16), and then rearranging terms, we find that the rescaled FPUT recurrence time for small  $S$  is given by

$$T_r = \frac{864S^2 - 5376\pi^2 S + 4096\pi^4}{405S^3 + 4104\pi^2 S^2 - 4992\pi^4 S + 2048\pi^6}. \quad (19)$$

This expression for  $T_r$  is shown in Fig. 4, along with the numerically determined rescaled FPUT recurrence time for large systems. It can be seen that Eq. (19) is an accurate expression for the rescaled recurrence time in the domain  $-12 \lesssim S \lesssim 4$ . Writing Eq. (19) to first order in  $S$  yields

$$T_r = \frac{2}{\pi^2} + \frac{9}{4\pi^4} S + \mathcal{O}(S^2) \sim 0.2026 + 0.0231S. \quad (20)$$

Comparing this to the numerical linear fits for small  $|S|$  given in Eqs. (12) and (14) shows excellent agreement.

### V. ROLE OF mKdV SOLITONS IN THE FPUT RECURRENCE

Since Zabusky and Kruskal’s semiquantitative explanation of the  $\alpha$ -FPUT recurrence in terms of solitons in the Korteweg–de Vries (KdV) equation,<sup>8</sup> it has been found that for  $R \gtrsim 4$  in the  $\alpha$ -FPUT chain,<sup>38</sup> the FPUT lattice recurrence time agrees with the recurrence time in the continuum.<sup>12</sup> Further, in the highly nonlinear regime, solitons dominate the time evolution of the KdV equation.<sup>34</sup> As the value of  $R$  increases, the number of solitons which form increases as well.<sup>39</sup> Before turning to an analytical estimate of the  $\beta$ -FPUT recurrence time in the highly nonlinear regime (large  $|S|$ ) in Sec. VI, we first investigate numerically the mKdV equation with initial conditions  $A\kappa\cos(\kappa\xi)/2$  to see whether the mKdV solitons contribute similarly to the FPUT recurrence in the  $\beta$ -FPUT chain, as the KdV solitons do in the  $\alpha$ -FPUT chain. We consider large  $N$  and set

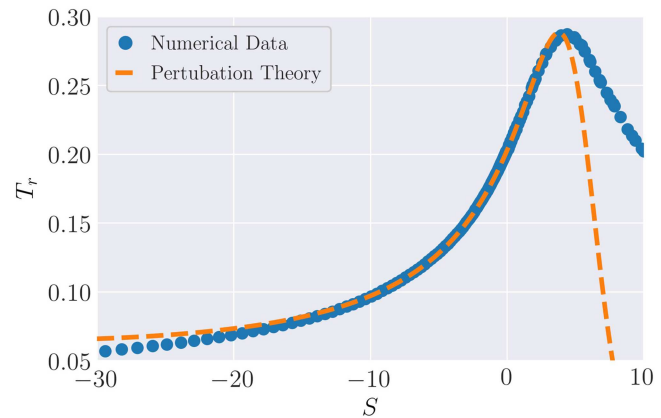
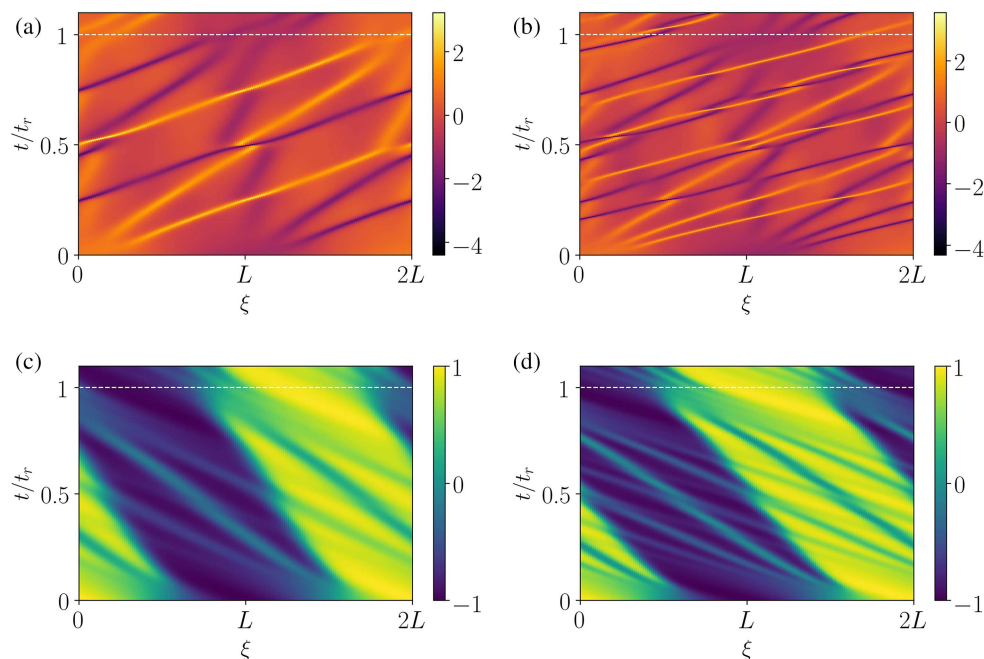


FIG. 4. The numerical data for the rescaled FPUT recurrence time plotted along with the results of Eq. (19) which was obtained analytically from the “shifted-frequency perturbation theory.”<sup>7</sup>

$|\beta| = 1$ , so the initial conditions can be written as  $\sqrt{|S|}L^{-1}\cos(\kappa\xi)$ . We note that the mKdV equation has both soliton and antisoliton solutions (see Appendix D), while the KdV equation has only soliton solutions.<sup>40</sup> We numerically solve the mKdV equation by first replacing the spatial derivatives with finite differences that have an error of  $\mathcal{O}(a^4)$ .<sup>41</sup> We then use the fourth-order Runge-Kutta method to find the time evolution. The lattice spacing is set to  $a = 1/(N + 1)$ , where  $N = 255$ , and the time step size  $dt = 0.1$ .

Figure 5 shows the numerically determined solutions of the mKdV equation in a “heat map” with the horizontal axis being the spatial coordinate, the vertical axis being the time coordinate, and the color indicating the amplitude of the field. The field  $\phi$  has been rescaled as  $\phi L|S|^{-1/2}$  such that 1 on the heat map corresponds to the maximum of the initial condition, and time,  $t$ , has been rescaled as  $t/t_r$ , where  $t_r$  is the FPUT recurrence time found in Sec. III for the given  $S$ . A horizontal white dashed line is graphed at  $t = t_r$  to emphasize the numerically determined FPUT recurrence time. We note that each value of  $S$  in parts (a)–(d) of Fig. 5 is large enough that the FPUT recurrence time is proportional to  $|S|^{-1/2}$ . As in Sec. III, we treat the  $\beta > 0$  and  $\beta < 0$  cases separately.

Figures 5(a) and 5(b) show  $S = 50$  and  $S = 100$ , respectively, with  $\beta = 1$  and  $N = 255$ . The spacetime diagrams both show that shortly after  $t = 0$ , solitons form on the bright background and antisolitons form on the dark background. Interestingly, for every soliton that forms, there is an antisoliton that forms with the same velocity and absolute value of the amplitude. In other words, the solitons and antisolitons come in pairs. At  $t = t_r$ , all of the solitons (antisolitons) overlap on the bright (dark) background. These values of  $\xi$  where the solitons (antisolitons) overlap correspond to roughly the same point where the (antisolitons) solitons initially formed on the (dark) bright background at  $t = 0$ ; therefore, there is a recurrence to the initial state. This is indeed similar to the mechanism which causes a recurrence of the initial state in the KdV equation.<sup>37</sup> Increasing  $S$  causes more solitons to form and does not affect the agreement of the recurrence time to that found on the lattice. However, for larger  $S$ , the increased number of solitons makes it less likely that they will all



**FIG. 5.** Shows a spacetime plot for the solution of the mKdV equation with an initial condition  $\sqrt{|S|}L^{-1}\cos(\kappa\xi)$  such that (a)  $S = 50$ , (b)  $S = 100$ , (c)  $S = -50$ , and (d)  $S = -100$ . The time axis is normalized by the numerically measured FPUT recurrence time on the lattice. The color of the “heat maps” corresponds to the value of  $\phi L |S|^{-1/2}$  at that point in space and time. For both signs of beta, solitons form for these large values of  $|S|$ .

successfully overlap at the same point, thereby weakening the recurrence. This is evident when  $S = 100$  at  $t = t_r$ , where there is a single soliton and antisoliton not overlapping with their respective others.

Considering next  $\beta < 0$ , Figs. 5(c) and 5(d) show  $S = -50$  and  $S = -100$ , respectively, where the only thing that has changed from the previous paragraph is the sign of  $\beta$ . Immediately after  $t = 0$ , once again we observe that pairs of antisolitons and solitons form. However, unlike the  $\beta > 0$  case, the antisolitons form on the bright background and the solitons on the dark background. Also, whereas the (anti)solitons for  $\beta > 0$  traveled to the right, opposite to the background which traveled to the left, the (anti)solitons for  $\beta < 0$  travel to the left along with the background. A more significant difference which affects the recurrence is that the  $\beta < 0$  solitary waves are always solitonlike when on the dark background and antisolitonlike when on the bright background (which is why  $-1 \leq \phi L |S|^{-1/2} \leq 1$ ). For example, a soliton that is initially on the dark background will always be solitonlike while on the dark background, but if it travels to the bright background, it becomes antisolitonlike. This did not happen for  $\beta > 0$ : Figs. 5(a) and 5(b) show that the (anti)solitons were essentially unaffected by their background. At the FPUT recurrence time, as for  $\beta > 0$ , all of the solitons overlap at one point and all of the antisolitons overlap at another point, which gives rise to approximately the initial conditions. However, the (anti)solitons that all meet at the same point at  $t = t_r$ , are not all the same (anti)solitons which formed together at the same point soon after  $t = 0$ . This is because the solitary waves change their “form” (soliton to antisoliton or antisoliton to soliton) based on their background. This difference in how

the solitons for  $\beta < 0$  interact with the background causes the recurrence to occur sooner. Indeed, for  $\beta > 0$ , close inspection of Figs. 5(a) and 5(b) shows that at  $t \sim t_r/2$ , there are two points in space,  $\xi = 0$  and  $\xi = L$ , where all of the solitons and antisolitons are overlapping. However, there are both solitons and antisolitons at these points, and therefore, a recurrence does not occur. This cannot happen in the  $\beta < 0$  case because there are never antisoliton-soliton interactions due to solitons (antisolitons) only ever existing on the dark (bright) background.

An important difference between positive and negative  $\beta$  that in fact provides an explanation for our numerical results is that the negative  $\beta$  mKdV has “kink” solutions, while the positive  $\beta$  case does not. As shown in previous studies (see Ref. 42) when a soliton interacts with a kink, the interaction causes the soliton to flip signs, thereby becoming an antisoliton. Therefore, given the numerical results, we argue that the background for the  $\beta < 0$  mKdV equation becomes a traveling kink-antikink. This is further supported by the form the background takes for negative  $\beta$ : nearly a constant value until it very quickly changes from bright to dark or dark to bright. In addition, this interpretation is also supported by the observation that negative  $\beta$  solitons and the background both undergo a phase shift when the soliton changes its background, just as in soliton-kink interactions.<sup>43</sup>

## VI. ANALYTICS IN THE HIGHLY NONLINEAR REGIME

In the highly nonlinear regime of the  $\alpha$ -FPUT chain, the FPUT recurrence time was analytically estimated from the velocities of the

KdV solitons, both neglecting<sup>37</sup> and including<sup>34,35</sup> phase shifts due to soliton-soliton interactions. As seen from the numerics in Sec. V, in the highly nonlinear regime of the  $\beta$ -FPUT chain, the recurrence of the initial state in the mKdV equation is also due to the solitons and antisolitons overlapping in their initial configuration. In this section, we seek an analytic estimate of the FPUT recurrence time by considering the soliton velocities. To do so, we first rewrite the mKdV equation in the “Lax pair” formalism<sup>44</sup>

$$\mathcal{L}_\tau = [\mathcal{A}, \mathcal{L}], \tag{21}$$

where  $[\cdot, \cdot]$  is the commutator and the Lax pair ( $\mathcal{L}$  and  $\mathcal{A}$ ) is given by<sup>45</sup>

$$\mathcal{L} \equiv i \begin{pmatrix} 1 & 0 \\ 0 & -1 \end{pmatrix} \partial_\xi - \frac{i\phi}{\sqrt{6b\zeta}} \begin{pmatrix} 0 & 1 \\ 1 & 0 \end{pmatrix}, \tag{22}$$

$$\begin{aligned} \mathcal{A} \equiv & -4\zeta \begin{pmatrix} 1 & 0 \\ 0 & 1 \end{pmatrix} \partial_\xi^3 - b \begin{pmatrix} \phi^2 & -\phi_\xi \sqrt{6b\zeta} \\ \phi_\xi \sqrt{6b\zeta} & \phi^2 \end{pmatrix} \partial_\xi \\ & - \frac{b}{2} \begin{pmatrix} 2\phi\phi_\xi & -\phi_{\xi\xi} \sqrt{6b\zeta} \\ \phi_{\xi\xi} \sqrt{6b\zeta} & 2\phi\phi_\xi \end{pmatrix}. \end{aligned} \tag{23}$$

The eigenvalue problem  $\mathcal{L}\vec{\psi}(\xi) = \sqrt{E}\vec{\psi}(\xi)$  is a 1 + 1 dimensional Dirac equation

$$\pm i(\psi_\pm)_\xi - \frac{i\phi}{\sqrt{6b\zeta}}\psi_\mp = \sqrt{E}\psi_\pm, \tag{24}$$

which has been used to show that the mKdV equation can be solved exactly by the inverse scattering transform.<sup>46</sup> Introducing the variables  $\Psi_\pm = \psi_- \pm i\psi_+$ , we can rewrite this Dirac equation as two Schrödinger equations<sup>47</sup>

$$-(\Psi_\pm)_{\xi\xi} + \left(-\frac{b}{6\zeta}\phi^2 \pm i\frac{1}{\sqrt{6b\zeta}}\phi_\xi\right)\Psi_\pm = E\Psi_\pm. \tag{25}$$

We note that Eq. (25) represents the corresponding Schrödinger equations of the KdV equation written in terms of the solutions to the mKdV equation through the Miura transform.<sup>48</sup> Notice, however, that the Hamiltonians in the Schrödinger equations for  $\beta > 0$  are non-hermitian! However, if  $\phi(\xi) = \phi(-\xi)$ , then the potential is parity-time ( $\mathcal{PT}$ ) symmetric and the spectra,  $E$ , can still be entirely real.<sup>49–51</sup>

Let us point out that  $E$  is a “time-independent” parameter and  $\phi$  satisfies the mKdV equation at “any” fixed time. Therefore, we can fix time to when the solitons have formed and then solve for  $E$  in terms of their velocities. Then, we can go back to  $\tau = 0$  and relate the solitons’ velocities to the parameters in the  $\beta$ -FPUT chain. If we neglect any phase shifts due to soliton-soliton, antisoliton-soliton, and antisoliton-antisoliton interactions, the FPUT recurrence occurs when the difference in speed between two consecutive (anti)solitons multiplied by the FPUT recurrence time is equal to  $2L$  for  $\beta > 0$  and  $L$  for  $\beta < 0$ . The factor of two difference comes from the numerical results presented in Sec. V. For  $\beta > 0$ , at the FPUT recurrence time, every initially formed soliton will be overlapping at about the same point, and, therefore, consecutive solitons, due to periodic boundary conditions, will be spaced out by the length of the space,  $2L$ . For  $\beta < 0$ , close inspection of Figs. 5(c) and 5(d) shows that at the

FPUT recurrence time, the spacing between the first and second soliton will instead be the distance between the two overlapping points, which from the numerics is half of the space,  $L$ . This is a direct consequence of the background for negative  $\beta$  becoming a kink-antikink, as discussed at the end of Sec. V.

Denoting the difference in speed between the  $(n + 1)$ st and the  $n$ th soliton by  $\Delta v$ , the FPUT recurrence time for the mKdV equation is, therefore, given by

$$\tau_r = \frac{(b + 3)L}{2\Delta v}. \tag{26}$$

The numerical coefficient is chosen such that for  $\beta > 0$  ( $\beta < 0$ ), then  $b = 1$  ( $b = -1$ ) and it takes the value 2 (1).

Since we are neglecting phase shifts due to the soliton interactions, we only need to consider the one-soliton solution of the mKdV equation on the real line. Furthermore, we only need to keep track of the solitons; since each soliton is paired with an antisoliton, when the solitons are distributed in space such that the FPUT recurrence occurs, so will be the antisolitons. Appendix D shows the explicit form of the soliton solutions for our normalization of the mKdV equation and also shows that for both positive and negative  $\beta$ , the difference in speed between consecutive solitons,  $\Delta v \equiv |v_{n+1} - v_n|$ , is

$$\Delta v = 4\zeta |E_{n+1} - E_n|. \tag{27}$$

Now considering  $\tau = 0$ , using the initial conditions given in Sec. II, the corresponding stationary Schrödinger equation is

$$-(\Psi_\pm)_{\xi\xi} + \left(-b\frac{\kappa^2 A^2 \cos^2(\kappa\xi)}{24\zeta} \mp \frac{i}{\sqrt{b}} \frac{\kappa^2 A \sin(\kappa\xi)}{2\sqrt{6\zeta}}\right)\Psi_\pm = E\Psi_\pm. \tag{28}$$

We proceed (following Toda<sup>37</sup>) by making the harmonic approximation and Taylor expanding to second order in  $\xi$ . Focusing first on  $\beta > 0$ , we expand about zero and, after some algebraic manipulations, find that the Schrödinger equation becomes

$$-(\Psi_\pm)_{\xi\xi} + \frac{A^2 \kappa^4}{24\zeta} \left(\xi \mp i\frac{\sqrt{6\zeta}}{\kappa A}\right)^2 \Psi_\pm = \left(E + \frac{\kappa^2 A^2}{24\zeta} - \frac{\kappa^2}{4}\right)\Psi_\pm, \tag{29}$$

which is a shifted quantum harmonic oscillator. Despite the shift being an imaginary number, because the boundary conditions are the same as if the shift were a real number, the multiplicative constant on the right-hand side is equal to the spectra of the harmonic oscillator<sup>52</sup>

$$E_n + \frac{\kappa^2 A^2}{24\zeta} - \frac{\kappa^2}{4} = \frac{A\kappa^2}{\sqrt{6\zeta}} \left(n + \frac{1}{2}\right), \tag{30}$$

with the index  $n$  labeling the solitons. Therefore, from Eqs. (26) and (27), the recurrence time is given by

$$\tau_r = \frac{L}{A\kappa^2} \sqrt{\frac{3}{2\zeta}}. \tag{31}$$

Rewriting all of the mKdV parameters in terms of the  $\beta$ -FPUT chain’s parameters, the rescaled recurrence time is found to be

$$T_r = \frac{2\sqrt{6}}{\pi^2 \sqrt{|\beta|} A}. \tag{32}$$

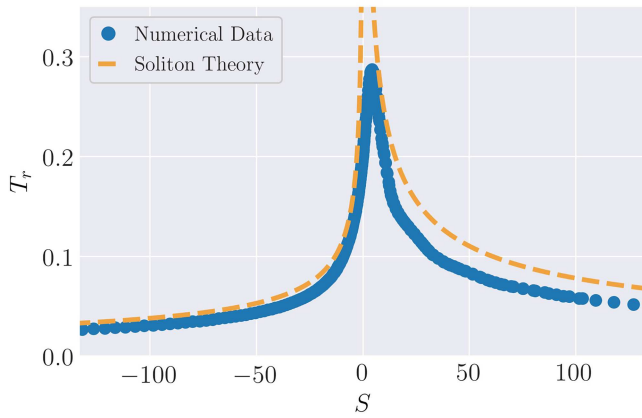


**FIG. 6.** A comparison of the numerically generated rescaled recurrence time and analytical expressions obtained from the noninteracting soliton approximations, which are given by Eqs. (33) and (36).

Using Eq. (A4) in the appendix, we can express the amplitude in terms of the parameter  $S$  in the large  $N$  limit and find

$$T_r = \frac{\sqrt{6}}{\pi} |S|^{-1/2}. \tag{33}$$

For the  $\beta < 0$  case, we expand about  $\xi = \pm\pi/(2\kappa)$  and the corresponding Schrödinger equation becomes

$$-(\Psi_{\pm})_{\xi\xi} + \frac{(A^2 + A\sqrt{6\zeta})\kappa^4}{24\zeta} \left(\xi \mp \frac{\pi}{2\kappa}\right)^2 \Psi_{\pm} = \left(E + \frac{\kappa^2 A}{2\sqrt{6\zeta}}\right) \Psi_{\pm}. \tag{34}$$

Therefore, for  $\beta < 0$ , the spectra follows

$$E_n + \frac{\kappa^2 A}{2\sqrt{6\zeta}} = \kappa^2 \sqrt{\frac{A^2 + A\sqrt{6\zeta}}{6\zeta}} \left(n + \frac{1}{2}\right), \tag{35}$$

and carrying through the calculation as done for  $\beta > 0$ , we find

$$T_r = \frac{3\sqrt{2}}{\pi\sqrt{12|S| + \pi\sqrt{6|S|}}}. \tag{36}$$

Figure 6 shows these calculated expressions along with the numerical data. Thus, we can see that for large  $|S|$ , the rescaled recurrence time goes like  $|S|^{-1/2}$ , as predicted by the numerics in Sec. III. The factor in front of  $|S|^{-1/2}$  for  $\beta > 0$  ( $\beta < 0$ ) is about 1.33 (1.27) times larger than the numerical factor in Eq. (13) [Eq. (15)]. This discrepancy is due to the harmonic approximation used to simplify Eq. (28) along with neglecting phase shifts in our calculation. We note that Wedding and Jäger performed similar calculations with the KdV equation, where they approximated  $\cos(x) \sim 4 \operatorname{sech}^2(x/\sqrt{8}) - 3$  and included first-order corrections to the recurrence time due to phase shifts.<sup>35</sup> Such a calculation should improve the multiplicative constant but is outside the scope of the current work.

### VII. EXISTENCE OF FPUT RECURRENCES

After understanding the scaling of the FPUT recurrence time as functions of  $E$ ,  $\beta$ , and  $N$ , we now explore which values of these

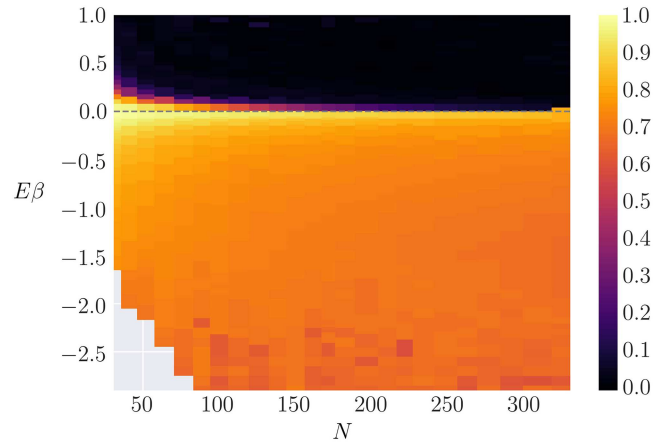


**FIG. 7.** A plot of  $E_1^{\min/E}$ , as a function of both  $N$  and  $E\beta$ . This represents the energy that never leaves the first normal mode for  $t < t_{\max}$  and is, therefore, not considered when computing shareable energy. The gray area represents systems that blow up before  $t_r$ .

parameters cause the FPUT recurrences to form. To compare the formation of an FPUT recurrence with an absence thereof, we investigate  $E_1^{\max}$ , the maximum energy in the first normal mode on the interval  $0.5t_r < t < 1.5t_r$ , with  $t_r$  given by the numerical scalings established in Sec. III. We will denote the time at which  $E_1^{\max}$  occurs as  $t_{\max}$ . When an FPUT recurrence forms, we expect  $t_{\max}$  to be the precise value of  $t_r$ .

To quantify the formation of an FPUT recurrence, we look at the proportion of “shareable energy” in the first normal mode at  $t = t_{\max}$ . We define shareable energy as  $\mathcal{E}(t) \equiv E_1(t) - E_1^{\min}$ , where  $E_1^{\min}$  is the minimum energy present in the first normal mode in the interval  $0 < t < t_{\max}$ .  $\mathcal{E}$  is defined this way, so it does not include the energy that is locked in the first normal mode. This is necessary to compare  $\beta < 0$  and  $\beta > 0$  because, as shown in Fig. 7, while most of the energy initially leaves the first normal mode at some time in the region  $0 < t < t_r$  for  $\beta > 0$  (as indicated by the black region), nearly 70% of it stays in the first normal mode for  $\beta < 0$  (as indicated by the orange colored region).

When an FPUT recurrence forms, we expect the proportion of shareable energy at  $t_{\max}$ ,  $\mathcal{E}(t_{\max})/\mathcal{E}(0)$ , to be nearly 1, whereas when no recurrence forms, the proportion of shareable energy should be much smaller than 1. Figure 8 is a heat map of  $\mathcal{E}(t_{\max})/\mathcal{E}(0)$  for the same values of  $E\beta$  and  $N$  as Fig. 7. It is clear that for large  $N$ , there is a critical value of  $E\beta$ , not  $S$ , where recurrences stop forming. Considering  $63 \leq N \leq 330$ , for  $\beta > 0$ , this  $E\beta_c^+ = 0.53 \pm .035$  whereas for  $\beta < 0$ ,  $E\beta_c^- = -2.43 \pm .055$  (95% confidence interval). Surprisingly, the magnitude of  $E\beta_c^-$  is almost five times greater than the magnitude of  $E\beta_c^+$ , meaning FPUT recurrences exist for much higher initial energies in the negative  $\beta$  case. It can be seen from Eq. (B11) in the appendix that for large  $N$ , the  $\beta < 0$  model can experience blowup for initial  $E\beta \lesssim -0.25$ . It is interesting to note that for  $\beta < 0$ , FPUT recurrences exist for initial energies up to nearly 10 times the energy above which blowup is possible.

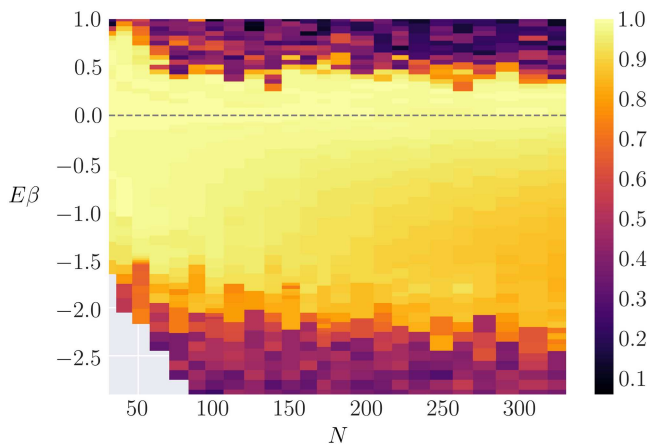


**FIG. 8.** A “heat map” of the “quality” of recurrences in the  $\beta$  FPUT model, for various system sizes  $N$  and initial conditions of constant  $E\beta$  in the first normal mode. The quantity plotted is  $\mathcal{E}(t_{\max})/\mathcal{E}(0)$ . This quantity represents the proportion of “shareable” energy that returns to the initial conditions. The gray area represents systems that blow up before  $t_r$ .

We can explain why the critical value at which FPUT recurrences stop forming is dependent on the energy but not the system size for large  $N$  by considering the so-called “metastable state,” which is an out-of-equilibrium quasistationary state that prevents (for a given period of time) the system from thermalizing.<sup>53</sup> Indeed, previous numerical investigations by Livi and Ruffo<sup>54</sup> for  $\beta > 0$  used the spectral entropy to show that at a fixed time and large  $N$ , the metastable state breaks down at an  $N$ -independent value  $E\beta_c^+ \sim \mathcal{O}(10^{-1})$ . Later, De Luca *et al.* used their four-mode subsystem to show analytically that for  $S \gg 1$  in the  $\beta > 0$  FPUT chain,  $E\beta_c^+ = 0.28$  is a critical energy for the diffusion of energy from low to high normal modes.<sup>18</sup> There has yet to be a study, at least to our knowledge, on these subjects for  $\beta < 0$ . Nevertheless, we would expect, given the numerics presented in Fig. 8, that the explanation would be similar. These results suggest that in the thermodynamic limit ( $N \rightarrow \infty$ ), where  $E \rightarrow \infty$  due to extensivity, FPUT recurrences will never form. We stress that this involves the breakdown of the metastable state, not the timescale to equipartition. Indeed, previous studies have found that the time it takes to achieve energy equipartition is dependent on the energy density,  $E\beta/N$ .<sup>55</sup> The same Livi and Ruffo study<sup>54</sup> indeed found that at a fixed time, energy equipartition is achieved at a critical value of  $E\beta/N$ .

While it appears that the disappearance of the FPUT recurrences corresponds to the breakdown of the metastable state, it is unclear what causes the metastable state to break down. We note that because the recurrences scale polynomially in time with the system size, Arnold diffusion does not play a role since, as proven by Nekhoroshev, it occurs on exponential time scales.<sup>56</sup> However, a possible explanation may come from considering the Kolmogorov–Arnold–Moser (KAM) theorem, relating the disappearances of the FPUT recurrences with the breakdown of KAM tori in phase space. Indeed, as shown by Ref. 57, the KAM theorem is indeed

applicable to FPUT, however, such rigorous application has thus far only been for small system sizes.

To ensure that our results are not a numerical artifact, we have confirmed that the numerics preserve time-reversal symmetry at, and slightly above, the critical value of  $E\beta$ . For  $\beta < 0$ , our results were time-reversible for all  $E\beta$  and  $N$ , with a time step size  $dt = 0.1$ . However, for  $\beta > 0$ , for large  $N$  and  $E\beta \gg E\beta_c^+$ , we were not able to ensure time reversibility with our allotted computational resources. This is due to the exponential instabilities that have been noted in other studies for  $\beta > 0$ <sup>16,17</sup> and has been explicitly studied as well in Ref. 15. We have confirmed that lowering the time step size, even if it is not small enough to ensure time reversibility, does not change the qualitative properties of Fig. 8.

### VIII. CONCLUSIONS AND DISCUSSION

Despite the comprehensive studies FPUT recurrences in the  $\alpha$ -FPUT chain have received in the past, there has not previously been a similarly comprehensive study of the FPUT recurrences in the  $\beta$ -FPUT chain. Using both numerical and analytical methods, we have examined these FPUT recurrences for both  $\beta < 0$  and  $\beta > 0$  in the  $\beta$ -FPUT chain and its continuum limit, the modified Korteweg–de Vries (mKdV) equation. Our results establish that the rescaled FPUT recurrence time  $T_r = t_r/(N + 1)^3$  is, for large  $N$ , completely described by the parameter  $S \equiv E\beta(N + 1)$ , and we have investigated the dependence of the FPUT recurrences on this and other lattice parameters.

For small  $|S|$ , the lattice is in a nearly linear regime. By numerically integrating the lattice model,  $T_r$  was found to transition smoothly between  $\beta < 0$  and  $\beta > 0$  as a function of  $S$ . Interestingly, the maximum value of  $T_r$  is located at  $S \sim 4.2$ . Using the shifted-frequency perturbation theory, we extended results from Ref. 7 and found a closed form for  $T_r$ , given in Eq. (19), which becomes a function of only  $S$  with an error of order  $\mathcal{O}((N + 1)^{-2})$ . This expression was found to accurately describe  $T_r$  for  $-12 \lesssim S \lesssim 4$ .

In the highly nonlinear regime (large  $|S|$ ), our numerical investigations revealed that for both  $\beta < 0$  and  $\beta > 0$ ,  $T_r \propto |S|^{-1/2}$ . However, the numerically fitted constant for  $\beta > 0$  was 0.5862, while it was 0.3078 for  $\beta < 0$ , and  $T_r$  followed this power-law when  $S \gtrsim 30$  and  $S \lesssim -12$ . We then went to the continuum limit and numerically investigated the role of mKdV antisolitons and solitons in the recurrence to the initial state. We found that as in the continuum limit of the  $\alpha$ -FPUT chain, solitons form and strongly influence the temporal evolution in the highly nonlinear regime. In this soliton-dominated regime, we found that  $T_r \propto |S|^{-1/2}$  agrees well with the recurrence time in the continuum. Furthermore, the recurrence was found to occur sooner for negative  $\beta$  due to soliton-kink interactions that do not occur for positive  $\beta$ . Finally, in the highly nonlinear regime, we estimated the FPUT recurrence time analytically by considering the velocities of the solitons and correctly replicated the  $|S|^{-1/2}$  power-law scaling of the rescaled FPUT recurrence time for both  $\beta < 0$  and  $\beta > 0$ .

Lastly, we concluded our study with investigations into which lattice parameters cause FPUT recurrences to form. We found that for large enough  $N$ , there is a critical value of  $E\beta$  above which FPUT recurrences do not form. The energies are, for  $\beta < 0$  and  $\beta > 0$ , respectively,  $E\beta_c^- = -2.43 \pm 0.055$  and  $E\beta_c^+ = 0.53 \pm 0.035$ , which

are surprisingly quite different. This critical value of  $E\beta$  has been associated with the breakdown/lack of formation of the metastable state. Another interesting result of this section was the discovery that while nearly all of the energy leaves the first normal mode before  $t_{\max}$  for  $\beta > 0$ , roughly 70% of the energy remains “locked” in the first normal mode up to  $t_{\max}$  for  $\beta < 0$ .

While there have been numerous studies on the stability and localizing properties of  $q$ -breathers<sup>9,58–60</sup> and  $q$ -tori,<sup>10,61</sup> there has yet to be a quantitative comparison of their periods to the FPUT recurrence time. The results presented here for the  $\beta$ -FPUT chain and those from Ref. 14 for the  $\alpha$ -FPUT chain provide an opportunity for a detailed study of this important open question.

The results of the current study also strongly suggest that the  $\beta$ -FPUT chain needs to be further investigated for  $\beta < 0$  with energy small enough to avoid blowup. Just as the FPUT recurrences behaved and scaled differently based on the sign of  $\beta$ , we expect other features of the dynamics to change with the sign of  $\beta$ . This includes the timescale to energy equipartition, which has been extensively studied in the  $\beta > 0$  case,<sup>18,55,62–64</sup> and also the intermittent dynamics at equilibrium. Recent studies revealed that the equilibrium dynamics in the  $\alpha$ -FPUT chain has long excursions from the equilibrium manifold due to sticky regions of phase space caused by  $q$ -breathers.<sup>65</sup>

An open question regarding the FPUT recurrence phenomena is how their scaling and existence depend on which normal mode(s) are initially excited. We have done preliminary work on this question in the  $\beta$ -FPUT chain and considered both second normal mode and first plus second normal mode initial conditions. Our preliminary results showed no qualitative difference: there were recurrences and other higher-order recurrences in both cases, which is why we considered only first normal mode initial conditions in this study. While we have evidence that this is true for low normal modes, we would expect striking differences from high normal mode (e.g., optical modes) initial conditions where previous studies have shown the existence of chaotic breathers.<sup>66</sup>

As a final remark, we recall the comment in our introduction that the dynamics of a one-dimensional Bose gas in the quantum rotor regime maps onto the  $\beta$ -FPUT chain with  $\beta < 0$ .<sup>19</sup> This suggests that our results may be of interest in studies of ultracold bosons confined in optical lattices.

## ACKNOWLEDGMENTS

We thank Felix Izrailev for stimulating discussions and Mark Ablowitz for valuable insights into the solutions of the mKdV equation. S.D.P. and K.A.R. are grateful for support from the Boston University’s Undergraduate Research Opportunities Program. Finally, we thank Boston University’s Research Computing Services for their computational resources.

## APPENDIX A: RELATIONSHIP BETWEEN ENERGY AND COORDINATE SPACE INITIAL AMPLITUDES

The initial condition in real space considered in this study is  $q_n = A \sin(n\pi/(N+1))$ . From the canonical transformation, Eq. (2), the initial normal mode coordinate is, therefore,  $Q_k(0) = A\delta_{1,k}\sqrt{(N+1)/2}$ . Using this initial condition and considering the Hamiltonian in normal mode coordinates, Eq. (3), the total

energy of the  $\beta$ -FPUT chain is

$$E = \frac{\omega_1^2 A^2 (N+1)}{4} \left( 1 + \frac{3b}{8} \omega_1^2 A^2 |\beta| \right). \quad (\text{A1})$$

Noting that  $S \equiv E\beta(N+1)$  is the relevant parameter in the scaling of the  $\beta$ -FPUT recurrences, we rewrite Eq. (A1) as

$$|S| = \frac{A^2 \omega_1^2 |\beta| (N+1)^2}{4} \left( 1 + \frac{3b |\beta| \omega_1^2 A^2}{8} \right). \quad (\text{A2})$$

Solving for  $A$ , and taking only the positive amplitude, we find

$$A = \left( \frac{\pi}{2(N+1)} \right) \sqrt{\frac{-1 + \sqrt{1 + 6b |S| (N+1)^{-2}}}{3b |\beta|}}. \quad (\text{A3})$$

As we are interested in the limit of large  $N$ , we note that

$$A = \frac{2}{\pi} \sqrt{\frac{|S|}{|\beta|}} + \mathcal{O}\left(\frac{1}{(N+1)^2}\right) \quad (\text{A4})$$

## APPENDIX B: SMALL TO LARGE SYSTEM SIZE THRESHOLD FOR $\beta < 0$

It has been shown that in the  $\alpha$ -FPUT chain the threshold for a system to be large enough to be described by its continuum limit is correlated to instabilities due to the potential being unbounded.<sup>38</sup> When  $\beta < 0$ , the system is unbounded and thus we expect a similar threshold to exist. Letting  $\Delta_n \equiv q_n - q_{n-1}$  and setting  $\ddot{q} = \dot{q} = 0$  in Eq. (6) with  $\beta < 0$ , we find that the extrema satisfy

$$\Delta_n (1 - |\beta| \Delta_n^2) = \Delta_{n+1} (1 - |\beta| \Delta_{n+1}^2), \quad (\text{B1})$$

which is essentially a cubic equation for  $\Delta_{n+1}$  in terms of  $\Delta_n$ . Letting  $\Delta_n \equiv \Xi$  and solving for  $\Delta_{n+1}$ , we find the three roots to be

$$\Delta_{n+1} = \Xi, \quad (\text{B2})$$

$$\Delta_{n+1} \equiv \Delta^{(+)} = \frac{-\Xi |\beta| + \sqrt{|\beta| (4 - 3\Xi^2 |\beta|)}}{2|\beta|}, \quad (\text{B3})$$

$$\Delta_{n+1} \equiv \Delta^{(-)} = \frac{-\Xi |\beta| - \sqrt{|\beta| (4 - 3\Xi^2 |\beta|)}}{2|\beta|}. \quad (\text{B4})$$

From the condition that

$$\sum_{n=1}^{N+1} \Delta_n = 0 \quad (\text{B5})$$

and letting there be  $j_1$  springs with  $\Delta^{(+)}$ ,  $j_2$  springs with  $\Delta^{(-)}$  and  $N+1-j_1-j_2$  with  $\Xi$ , Eq. (B5) becomes

$$j_1 \Delta^{(+)} + j_2 \Delta^{(-)} + (N+1-j_1-j_2) \Xi = 0. \quad (\text{B6})$$

Solving for  $\Xi$ , we find

$$\Xi = \frac{\pm(j_1 - j_2) |\beta|^{-1/2}}{\sqrt{3(j_1^2 + j_2^2) + 3j_1 j_2 - 3(j_1 + j_2)(N+1) + (N+1)^2}}. \quad (\text{B7})$$

We want to choose  $j_1, j_2$ , and the  $\pm$  sign such that the energy

$$E_c = j_1 \left( \frac{1}{2} (\Delta_n^{(+)})^2 - \frac{|\beta|}{4} (\Delta_n^{(+)})^4 \right) + j_2 \left( \frac{1}{2} (\Delta_n^{(-)})^2 - \frac{|\beta|}{4} (\Delta_n^{(-)})^4 \right) + (N + 1 - j_1 - j_2) \left( \frac{1}{2} \Xi^2 - \frac{|\beta|}{4} \Xi^4 \right) \quad (B8)$$

is minimized, which will give us a lower estimate. The expression above is invariant under any of the  $\Delta_n^{(+)}, \Delta_n^{(-)}$ , or  $\Xi$  variables picking up an overall minus sign. We also note that the expression for  $\Xi$  picks up an overall minus sign when  $j_1$  and  $j_2$  are switched. Therefore, switching  $j_1$  with  $j_2$  in Eq. (B8) also causes  $\Delta_n^{(-)}$  and  $\Delta_n^{(+)}$  to switch, leaving the form for  $E_c$  unchanged. Therefore, without loss of generality, we can set  $j_2 = 0$ . With this, the energy is minimized if we choose the  $\pm$  sign in  $\Xi$  to be + and also chose  $j_1 = 1$ . The minimized energy threshold becomes

$$E_c = \frac{N^4 - N + 1}{4|\beta|(N^2 - N + 1)^2}. \quad (B9)$$

In terms of  $S_c \equiv E_c \beta (N + 1)$ , we have

$$|S_c| = \frac{(N + 1)(N^4 - N + 1)}{4(N^2 - N + 1)^2}. \quad (B10)$$

For large  $N$ , this goes like

$$|S_c| \sim \frac{N + 3}{4} + \mathcal{O}\left(\frac{1}{N}\right) \quad (B11)$$

Hence, for  $N \gtrsim 4|S| - 3$ , we expect the lattice to be considered large and thus to behave similarly to its continuum limit—the mKdV equation. Figure 9 shows the dependence of the rescaled FPUT recurrence times on  $S$ , as presented in Sec. III but also includes the numerical data that do not agree with the common trend shown in

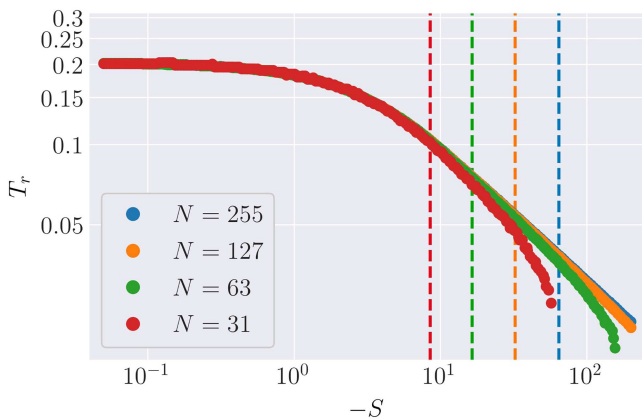


**FIG. 9.** Shows the rescaled recurrence time as a function of  $S$ , but, unlike Fig. 3, also includes including data points when the system is too small and does not follow the large  $N$  trend. The vertical lines are the critical  $S$  between a small and large system which is given by Eq. (B10).

Fig. 3. As discussed in the main text, this disagreement arises because the system sizes are too small to be described by the continuum limit. The vertical lines represent the critical values of  $S$  that separate the “small” and “large” systems, as given by Eq. (B10). These lines are plotted for the same system sizes  $N = 31, 63, 127$ , and  $255$  and follow the same color coding as the numerical data. The numerical data start to “peel-off” from its larger counterparts at values that are close to the vertical lines. Close inspection of the numerical data shows that disagreements with the larger counterparts occurs for  $N = 31$  at  $S_c \sim 7.1$ ,  $N = 63$  at  $S_c \sim 14.6$ , and  $N = 127$  at  $S_c \sim 29.4$ . This confirms that, as in the  $\alpha$ -FPUT chain,<sup>38</sup> there is indeed a correlation between the instabilities that arise due to saddle points and the small to large system size threshold.

### APPENDIX C: SHIFTED-FREQUENCY PERTURBATION THEORY

The underlying assumption of the shifted-frequency perturbation theory presented by Sholl and Henry in Ref. 7 is that each normal mode coordinate can be written as

$$Q_k = \sum_{j=0}^{\infty} \beta^j Q_{k,j}, \quad (C1)$$

and that there are nonlinear frequencies, defined by

$$\Omega_k^2 \equiv \omega_k^2 + \sum_{j=1}^{\infty} \beta^j \mu_{k,j}. \quad (C2)$$

The variables  $Q_{k,j}$  are found by inserting Eq. (C1) into the normal mode coordinate equations of motion

$$\ddot{Q}_k + \Omega_k^2 Q_k = - \sum_{i,j,l=1}^N C_{kijl} Q_i Q_j Q_l, \quad (C3)$$

where the  $\omega_k^2$  in front of the  $Q_k$  term on the left-hand side has been replaced by  $\Omega_k^2$ , but the coupling constant  $C_{kijl}$  is still given in terms of the linear frequencies, as given in Eq. (5). After this substitution, the  $\mu_{k,j}$ s, called the “frequency corrections,” are then chosen so as to eliminate secular terms.

Sholl and Henry calculated up to third-order corrections to  $Q_k$  for initial conditions  $Q_k(0) = \delta_{k,1}, P_k(0) = 0$ . We discussed the expression they found for the FPUT recurrence time in the  $\beta$ -FPUT chain in Sec. IV. Here, we restate their results for the frequency corrections of the first, third, and fifth nonlinear frequency

$$\mu_{1,1} = \frac{3}{4} C_{1111}, \quad (C4)$$

$$\mu_{1,2} = -\frac{3}{4} C_{1111} A_{1,1} + \frac{3}{4} C_{1,1,1,3} (3A_{3,2} + A_{3,3}), \quad (C5)$$

$$\mu_{3,1} = \frac{3}{2} C_{3311}, \quad (C6)$$

$$\begin{aligned} \mu_{3,2} = & \frac{3}{4A_{3,1}} [C_{3111} (2B_{1,4} + B_{1,5} + B_{1,6}) \\ & + C_{3311} (B_{3,5} + B_{3,6} - 4A_{3,1}A_{1,1}) \\ & + C_{3115} (2B_{5,5} + B_{5,6} + B_{5,7})], \end{aligned} \tag{C7}$$

$$\mu_{5,1} = \frac{3}{2} C_{5511}. \tag{C8}$$

The  $C_{kijl}$  are the coupling constants defined by Eq. (5), and the constants  $A_{ij}$  and  $B_{ij}$  are given by

$$A_{1,1} = \frac{C_{1111}}{32\Omega_1^2}, \tag{C9}$$

$$A_{3,2} = \frac{-3C_{1111}}{4(\Omega_3^2 - \Omega_1^2)}, \tag{C10}$$

$$A_{3,3} = \frac{-C_{1111}}{4(\Omega_3^2 - 9\Omega_1^2)}, \tag{C11}$$

$$A_{3,1} = -A_{3,2} - A_{3,3}, \tag{C12}$$

$$B_{1,4} = \frac{-3C_{1113}A_3}{2(\Omega_1^2 - \Omega_3^2)}, \tag{C13}$$

$$B_{1,5} = \frac{-3C_{1113}A_{3,1}}{4(\Omega_1^2 - (\Omega_3 - 2\Omega_1)^2)}, \tag{C14}$$

$$B_{1,6} = \frac{-3C_{1113}A_{3,1}}{4(\Omega_1^2 - (\Omega_3 + 2\Omega_1)^2)}, \tag{C15}$$

$$B_{3,5} = \frac{-3C_{3311}A_{3,1}}{4(\Omega_3^2 - (\Omega_3 - 2\Omega_1)^2)}, \tag{C16}$$

$$B_{3,6} = \frac{-3C_{3311}A_{3,1}}{(\Omega_3^2 - (\Omega_3 + 2\Omega_1)^2)}, \tag{C17}$$

$$B_{5,5} = \frac{3C_{5311}A_{3,1}}{2(\Omega_3^2 - \Omega_5^2)}, \tag{C18}$$

$$B_{5,6} = \frac{3C_{5311}A_{3,1}}{4((\Omega_3 - 2\Omega_1)^2 - \Omega_5^2)}, \tag{C19}$$

$$B_{5,7} = \frac{3C_{5311}A_{3,1}}{4((\Omega_3 + 2\Omega_1)^2 - \Omega_5^2)}. \tag{C20}$$

We note that constants  $B_{5,5}$ ,  $B_{5,6}$ , and  $B_{5,7}$  were never explicitly reported in Ref. 7. They are found by solving Eq. (22) in their manuscript, which is a differential equation whose solution is the second-order corrections of the 5th normal mode coordinate,  $Q_{5,2}$ . Doing so, we find that

$$\begin{aligned} Q_{5,2}(t) = & B_{5,1}\cos(\Omega_5 t) + B_{5,2}\cos(\Omega_1 t) + B_{5,3}\cos(3\Omega_1 t) \\ & + B_{5,4}\cos(5\Omega_1 t) + B_{5,5}\cos(\Omega_3 t) \\ & + B_{5,6}\cos((2\Omega_1 - \Omega_3)t) + B_{5,7}\cos((2\Omega_1 + \Omega_3)t), \end{aligned} \tag{C21}$$

where  $B_{5,5}$ ,  $B_{5,6}$ , and  $B_{5,7}$  are listed above, and  $B_{5,1}$ ,  $B_{5,2}$ ,  $B_{5,3}$ , and  $B_{5,4}$  are

$$B_{5,1} = -\sum_{n=2}^7 B_{5,n}, \tag{C22}$$

$$B_{5,2} = \frac{3(3A_{3,2} + A_{3,3})C_{5311}}{4(\Omega_1^2 - \Omega_5^2)}, \tag{C23}$$

$$B_{5,3} = \frac{3(A_{3,2} + 2A_{3,3})C_{5311}}{4(9\Omega_1^2 - \Omega_5^2)}, \tag{C24}$$

$$B_{5,4} = \frac{3A_{3,3}C_{5311}}{4(25\Omega_1^2 - \Omega_5^2)}. \tag{C25}$$

We note that in Eqs. (C8)–(C23), all of the nonlinear frequencies are calculated to first order in  $\beta$ .

#### APPENDIX D: SOLITONS IN THE mKdV EQUATION

In Sec. VI, we use the speed of the solitons which form in the continuum to find an approximate expression for the FPUT recurrence time on the lattice. In this Appendix, we restate known information in the literature about the one-soliton solutions of the mKdV equation given by Eq. (11). For simplicity, we will not include the arbitrary phase shifts  $\xi \rightarrow \xi + \xi_0$ .

The one-soliton solution on the real line is given by<sup>42,67</sup>

$$\phi = \frac{3\sqrt{2}(\phi_\infty^2 - v)}{\sqrt{3v - \phi_\infty^2} \cosh(\eta\sqrt{b(v - \phi_\infty^2)}) - \phi_\infty\sqrt{2}} + \phi_\infty, \tag{D1}$$

where  $\eta = \zeta^{-1/2}(\xi - b\tau)$  and  $b = \text{sgn}(\beta)$ . For  $\beta < 0$ , solitons (antisolitons) reside on a negative (positive) background, while for  $\beta > 0$ , solitons and antisolitons can be on both a positive or negative background. There are obvious restrictions on what value  $\phi_\infty$  can take given the soliton speed. For  $\beta > 0$ , the soliton exists for  $-\sqrt{v} < \phi_\infty < \sqrt{v}$ , while for  $\beta < 0$  it exists for  $-\sqrt{3v} < \phi_\infty < -\sqrt{v}$ . From this, it is clear that no one-soliton solutions exist at zero background for negative  $\beta$ . However, for positive  $\beta$ , we can set the background to zero and return to the well-known result<sup>40,46</sup>

$$\phi = \pm\sqrt{6v} \operatorname{sech}\left(\sqrt{\frac{v}{\zeta}}(\xi - v\tau)\right). \tag{D2}$$

Also, while it is not used in our results, we note that for  $\beta > 0$  there are also algebraic solitons<sup>68</sup>

$$\phi = \sqrt{v} \left(1 - \frac{12\zeta}{3\zeta + 2v(\xi - v\tau)^2}\right). \tag{D3}$$

While there are solitons in both the  $\beta > 0$  and  $\beta < 0$  mKdV equations, the  $\beta < 0$  case also has kinks. The one-kink solution is<sup>69</sup>

$$\phi = \sqrt{3v} \tanh\left(\sqrt{\frac{v}{\zeta}}(\xi + v\tau)\right). \tag{D4}$$

The speed,  $v$ , of the soliton given in Eq. (D1) has been expressed in terms of the eigenvalue  $E$  in the corresponding Schrödinger equation given by Eq. (25) through the  $N$ -soliton solutions as<sup>42,67</sup>

$$v = \frac{\phi_\infty^2}{3} - 4b\zeta E. \tag{D5}$$

Important for the calculation presented in Sec. VI, the difference in the speed of consecutive solitons for both positive and negative  $\beta$  is, therefore, given by

$$\Delta v = 4\zeta |E_{n+1} - E_n|. \tag{D6}$$

## REFERENCES

- <sup>1</sup>E. Fermi, J. R. Pasta, S. Ulam, and M. Tsingou, "Studies of nonlinear problems, I," Los Alamos Report No. LA-1940, 1955.
- <sup>2</sup>J. Ford, "The Fermi-Pasta-Ulam problem: Paradox turns discovery," *Phys. Rep.* **213**(5), 271–310 (1992).
- <sup>3</sup>T. P. Weisert, *The Genesis of Simulation in Dynamics* (Springer-Verlag, New York, 1997).
- <sup>4</sup>G. P. Berman and F. M. Izrailev, "The Fermi-Pasta-Ulam problem: Fifty years of progress," *Chaos* **15**(1), 015104 (2005).
- <sup>5</sup>*Fermi-Pasta-Ulam Problem: A Status Report*, edited by G. Gallavotti (Springer-Verlag, Berlin, 2007).
- <sup>6</sup>J. Ford, "Equipartition of energy for nonlinear systems," *J. Math. Phys.* **2**(3), 387–393 (1961).
- <sup>7</sup>D. S. Sholl and B. I. Henry, "Recurrence times in cubic and quartic Fermi-Pasta-Ulam chains: A shifted-frequency perturbation treatment," *Phys. Rev. A* **44**(10), 6364–6374 (1991).
- <sup>8</sup>N. J. Zabusky and M. D. Kruskal, "Interaction of "solitons" in a collisionless plasma and the recurrence of initial states," *Phys. Rev. Lett.* **15**(6), 240–243 (1965).
- <sup>9</sup>S. Flach, M. V. Ivanchenko, and O. I. Kanakov, "*q*-Breathers and the Fermi-Pasta-Ulam problem," *Phys. Rev. Lett.* **95**, 064102 (2005).
- <sup>10</sup>H. Christodoulidi, C. Efthymiopoulos, and T. Bountis, "Energy localization on *q*-tori, long-term stability, and the interpretation of Fermi-Pasta-Ulam recurrences," *Phys. Rev. E* **81**, 016210 (2010).
- <sup>11</sup>N. J. Zabusky, "Phenomena associated with the oscillations of a nonlinear model string," in *Proceedings of the Conference on Mathematical Models in the Physical Sciences*, edited by S. Drobot (Prentice-Hall, Inc., Englewood Cliffs, New Jersey, 1963), pp. 99–133.
- <sup>12</sup>N. J. Zabusky, "Nonlinear lattice dynamics and energy sharing," *J. Phys. Soc. Jpn.* **26**(Suppl.), 196–202 (1969).
- <sup>13</sup>M. Toda, "mechanics and statistical Mechanics of nonlinear chains," *J. Phys. Soc. Jpn.* **26**(Suppl.), 235–237 (1969).
- <sup>14</sup>C. Y. Lin, C. G. Goedde, and S. Lichter, "Scaling of the recurrence time in the cubic Fermi-Pasta-Ulam lattice," *Phys. Lett. A* **229**(6), 367–374 (1997).
- <sup>15</sup>C. F. Driscoll and T. M. O'Neil, "Explanation of instabilities observed on a Fermi-Pasta-Ulam lattice," *Phys. Rev. Lett.* **37**(2), 69–72 (1976).
- <sup>16</sup>G. P. Drago and S. Ridella, "Some more observations on the superperiod of the non-linear FPU system," *Phys. Lett. A* **122**(8), 407–412 (1987).
- <sup>17</sup>S. D. Pace and D. K. Campbell, "Behavior and breakdown of higher-order Fermi-Pasta-Ulam-Tsingou recurrences," *Chaos* **29**(2), 023132 (2019).
- <sup>18</sup>J. De Luca, A. J. Lichtenberg, and M. A. Lieberman, "Time scale to ergodicity in the Fermi-Pasta-Ulam system," *Chaos* **5**(1), 283–297 (1995).
- <sup>19</sup>I. Danshita, R. Hipolito, V. Oganessian, and A. Polkovnikov, "Quantum damping of Fermi-Pasta-Ulam revivals in ultracold Bose gases," *Prog. Theor. Exp. Phys.* **2014**(4), 1–8 (2014).
- <sup>20</sup>G. Kopidakis, C. M. Soukoulis, and E. N. Economou, "Electron-phonon interactions and recurrence phenomena in one-dimensional systems," *Phys. Rev. B* **49**, 7036–7039 (1994).
- <sup>21</sup>N. N. Rosanov and N. V. Vysotina, "Recurrence for motion of solitons of the Bose-Einstein condensate in a dynamic trap," *J. Opt. Soc. Am. B* **32**(5), 20–24 (2015).
- <sup>22</sup>K. Abe and N. Satofuka, "Recurrence of initial state of nonlinear ion waves," *Phys. Fluids* **24**(6), 1045–1048 (1981).
- <sup>23</sup>V. Balasubramanian, A. Buchel, S. R. Green, L. Lehner, and S. L. Liebling, "Holographic thermalization, stability of anti-de Sitter space, and the Fermi-Pasta-Ulam paradox," *Phys. Rev. Lett.* **113**(7), 071601 (2014).
- <sup>24</sup>A. Biasi, B. Craps, and O. Evnin, "Energy returns in global AdS<sub>4</sub>," *Phys. Rev. D* **100**, 024008 (2019).
- <sup>25</sup>R. Hirota and K. Suzuki, "Studies on lattice solitons by using electrical networks," *J. Phys. Soc. Jpn.* **28**(5), 1366–1367 (1970).
- <sup>26</sup>H. Ikezi, "Experiments on ion-acoustic solitary waves," *Phys. Fluids* **16**(10), 1668–1675 (1973).
- <sup>27</sup>B. M. Lake, H. C. Yuen, H. Rungaldier, and W. E. Ferguson, "Nonlinear deep-water waves: Theory and experiment. Part 2. Evolution of a continuous wave train," *J. Fluid. Mech.* **83**(1), 49–74 (1977).
- <sup>28</sup>G. Van Simaey, P. Emplit, and M. Haelterman, "Experimental demonstration of the Fermi-Pasta-Ulam recurrence in a modulationally unstable optical wave," *Phys. Rev. Lett.* **87**(3), 33902 (2001).
- <sup>29</sup>M. M. Scott, B. A. Kalinikos, and C. E. Patton, "Spatial recurrence for nonlinear magnetostatic wave excitations," *J. Appl. Phys.* **94**(9), 5877–5880 (2003).
- <sup>30</sup>M. Wu and C. E. Patton, "Experimental observation of Fermi-Pasta-Ulam recurrence in a nonlinear feedback ring system," *Phys. Rev. Lett.* **98**(4), 047202 (2007).
- <sup>31</sup>D. Pierangeli, M. Flammini, L. Zhang, G. Marcucci, A. Agrat, P. Grinevich, P. Santini, C. Conti, and E. DelRe, "Observation of Fermi-Pasta-Ulam-Tsingou recurrence and its exact dynamics," *Phys. Rev. X* **8**(4), 041017 (2018).
- <sup>32</sup>D. S. Sholl, "Modal coupling in one-dimensional anharmonic lattices," *Phys. Lett. A* **149**(5–6), 253–257 (1990).
- <sup>33</sup>M. Ablowitz and H. Segur, *Solitons and the Inverse Scattering Transform* (Society for Industrial and Applied Mathematics, 1981).
- <sup>34</sup>A. R. Osborne and L. Bergamasco, "The solitons of Zabusky and Kruskal revisited: Perspective in terms of the periodic spectral transform," *Physica D* **18**(1–3), 26–46 (1986).
- <sup>35</sup>B. Wedding and D. Jäger, "Quantitative study of recurrence in Korteweg de Vries systems," *J. Appl. Phys.* **53**(8), 5377–5381 (1982).
- <sup>36</sup>J. Laskar and P. Robutel, "High order symplectic integrators for perturbed Hamiltonian systems," *Celestial Mech. Dyn. Astron.* **80**, 39–62 (2001).
- <sup>37</sup>M. Toda, "Studies of a non-linear lattice," *Phys. Rep.* **18**(1), 1–123 (1975).
- <sup>38</sup>C. Y. Lin, S. N. Cho, C. G. Goedde, and S. Lichter, "When is a one-dimensional lattice small?," *Phys. Rev. Lett.* **82**(2), 259–262 (1999).
- <sup>39</sup>A. Salupere, G. A. Maugin, J. Engelbrecht, and J. Kalda, "On the KdV soliton formation and discrete spectral analysis," *Wave Motion* **23**(1), 49–66 (1996).
- <sup>40</sup>N. J. Zabusky, "A synergetic approach to problems of nonlinear dispersive wave propagation and interaction," in *Nonlinear Partial Differential Equations* (Academic Press, 1967), pp. 223–258.
- <sup>41</sup>B. Fornberg, "Generation of finite difference formulas on arbitrarily spaced grids," *Math. Comput.* **51**(184), 699–699 (1988).
- <sup>42</sup>T. L. Perelman, A. K. Fridman, and M. M. El'Yashevich, "On the relationship between the N-soliton solution of the modified Korteweg-de Vries equation and the KdV equation solution," *Phys. Lett. A* **47**(4), 321–323 (1974).
- <sup>43</sup>L. R. T. Gardner, G. A. Gardner, and T. Geyikli, "Solitary wave solutions of the MKdV equation," *Comput. Methods Appl. Mech. Eng.* **124**(4), 321–333 (1995).
- <sup>44</sup>P. D. Lax, "Integrals of nonlinear equations of evolution and solitary waves," *Commun. Pure Appl. Math.* **21**(5), 467–490 (1968).
- <sup>45</sup>T. Aktosun, *Inverse Scattering Transform and the Theory of Solitons* (Springer, New York, NY, 2011), pp. 771–782.
- <sup>46</sup>M. Wadati, "The exact solution of the modified Korteweg-de Vries equation," *J. Phys. Soc. Jpn.* **32**(6), 1681 (1972).
- <sup>47</sup>G. L. Lamb, *Elements of Soliton Theory* (Wiley, 1980).
- <sup>48</sup>R. M. Miura, "Korteweg-de Vries equation and generalizations. I. A remarkable explicit nonlinear transformation," *J. Math. Phys.* **9**(8), 1202–1204 (1968).
- <sup>49</sup>C. M. Bender, "Introduction to  $\mathcal{PT}$ -symmetric quantum theory," *Contemp. Phys.* **46**(4), 277–292 (2005).
- <sup>50</sup>C. M. Bender, *PT Symmetry: In Quantum and Classical Physics* (WSPC, Europe, 2019).
- <sup>51</sup>M. Wadati, "Construction of parity-time symmetric potential through the soliton theory," *J. Phys. Soc. Jpn.* **77**(7), 074005 (2008).
- <sup>52</sup>M. Znojil, " $\mathcal{PT}$ -symmetric harmonic oscillators," *Phys. Lett. A* **259**(3–4), 220–223 (1999).
- <sup>53</sup>G. Benettin, A. Carati, L. Galgani, and A. Giorgilli, *The Fermi Pasta Ulam Problem and the Metastability Perspective*, Lecture Notes in Physics (Springer Verlag, Berlin, 2008), Vol. 728, p. 151.
- <sup>54</sup>R. Livi and S. Ruffo, *Equipartition Transition and Lyapunov Exponents in Closed Hamiltonian Systems* (World Scientific Publishing Co., 1992), pp. 113–123.
- <sup>55</sup>V. V. Lvov and M. Onorato, "Double scaling in the relaxation time in the  $\beta$ -Fermi-Pasta-Ulam-Tsingou model," *Phys. Rev. Lett.* **120**(14), 144301 (2018).
- <sup>56</sup>G. Benettin, L. Galgani, and A. Giorgilli, "A proof of Nekhoroshev's theorem for the stability times in nearly integrable Hamiltonian systems," *Celestial Mech.* **37**, 1–25 (1985).

- <sup>57</sup>B. Rink, "Symmetry and resonance in periodic FPU chains," *Commun. Math. Phys.* **218**, 665–685 (2001).
- <sup>58</sup>S. Flach, M. V. Ivanchenko, and O. I. Kanakov, "q-Breathers in Fermi-Pasta-Ulam chains: Existence, localization, and stability," *Phys. Rev. E* **73**(3), 1–14 (2006).
- <sup>59</sup>T. Penati and S. Flach, "Tail resonances of Fermi-Pasta-Ulam q-breathers and their impact on the pathway to equipartition," *Chaos*, **17**(2), 023102 (2007).
- <sup>60</sup>S. Flach, M. V. Ivanchenko, O. I. Kanakov, and K. G. Mishagin, "Periodic orbits, localization in normal mode space, and the Fermi-Pasta-Ulam problem," *Am. J. Phys.* **76**(4), 453–459 (2008).
- <sup>61</sup>H. Christodoulidi and C. Efthymiopoulos, "Low-dimensional q-tori in FPU lattices: Dynamics and localization properties," *Physica D* **261**, 92–113 (2013).
- <sup>62</sup>R. Livi, M. Pettini, S. Ruffo, M. Sparpaglione, and A. Vulpiani, "Equipartition threshold in nonlinear large Hamiltonian systems: The Fermi-Pasta-Ulam model," *Phys. Rev. A* **31**(2), 1039–1045 (1985).
- <sup>63</sup>L. Berchiolla, A. Giorgilli, and S. Paleari, "Exponentially long times to equipartition in the thermodynamic limit," *Phys. Lett. A* **321**(3), 167–172 (2004).
- <sup>64</sup>G. Benettin and A. Ponno, "Time-scales to equipartition in the Fermi-Pasta-Ulam problem: Finite-size effects and thermodynamic limit," *J. Stat. Phys.* **144**(4), 793–812 (2011).
- <sup>65</sup>C. Danieli, D. K. Campbell, and S. Flach, "Intermittent many-body dynamics at equilibrium," *Phys. Rev. E* **95**(6), 1–5 (2017).
- <sup>66</sup>T. Dauxois, R. Khomeriki, F. Piazza, and S. Ruffo, "The anti-FPU problem," *Chaos* **15**(1), 015110 (2005).
- <sup>67</sup>G. Chanteur and M. Raadu, "Formation of shocklike modified Korteweg-de Vries solitons: Application to double layers," *Phys. Fluids* **30**(9), 2708–2719 (1987).
- <sup>68</sup>H. Ono, "Algebraic soliton of the modified Korteweg-de Vries equation," *J. Phys. Soc. Jpn.* **41**(5), 1817–1818 (1976).
- <sup>69</sup>H. Grosse, "Solitons of the modified KdV equation," *Lett. Math. Phys.* **8**(4), 313–319 (1984).